

The College at Brockport: State University of New York Digital Commons @Brockport

Biology Faculty Publications

Department of Biology

2009

The $\alpha 1H Ca^{2+}$ channel subunit is expressed in mouse jejunal interstitial cells of Cajal and myocytes

Simon J. Gibbons
Mayo Medical School

Peter R. Strege
Mayo Medical School


Sha Lei
Mayo Medical School

Jaime L. Roeder
Mayo Medical School

Amelia Mazzone
Mayo Medical School

See next page for additional authors

Follow this and additional works at: https://digitalcommons.brockport.edu/bio_facpub

 Part of the [Biology Commons](#), [Cell Biology Commons](#), [Gastroenterology Commons](#), and the [Molecular and Cellular Neuroscience Commons](#)

Repository Citation

Gibbons, Simon J.; Strege, Peter R.; Lei, Sha; Roeder, Jaime L.; Mazzone, Amelia; Ou, Yijun; Rich, Adam; and Farrugia, Gianrico, "The $\alpha 1H Ca^{2+}$ channel subunit is expressed in mouse jejunal interstitial cells of Cajal and myocytes" (2009). *Biology Faculty Publications*. 4.

https://digitalcommons.brockport.edu/bio_facpub/4

This Article is brought to you for free and open access by the Department of Biology at Digital Commons @Brockport. It has been accepted for inclusion in Biology Faculty Publications by an authorized administrator of Digital Commons @Brockport. For more information, please contact kmyers@brockport.edu.

Authors

Simon J. Gibbons, Peter R. Strege, Sha Lei, Jaime L. Roeder, Amelia Mazzone, Yijun Ou, Adam Rich, and Gianrico Farrugia

The α_{1H} Ca^{2+} channel subunit is expressed in mouse jejunal interstitial cells of Cajal and myocytes

Simon J. Gibbons^{a, b, c, *}, Peter R Strege^{a, b, c}, Sha Lei^{a, b, c}, Jaime L. Roeder^{a, b, c},
Amelia Mazzone^{a, b, c}, Yijun Ou^{a, b, c}, Adam Rich^d, Gianrico Farrugia^{a, b, c}

^aEnteric Neuroscience Program, Mayo Clinic College of Medicine, Rochester, MN, USA

^bDepartment of Physiology and Biomedical Engineering, Mayo Clinic College of Medicine, Rochester, MN, USA

^cMiles and Shirley Fiterman Center for Digestive Diseases, Mayo Clinic, Rochester, MN, USA

^dDepartment of Biological Sciences, SUNY Brockport, 350 New Campus Drive, Brockport, NY, USA

Q1

Abstract

T-type Ca^{2+} currents have been detected in cells from the external muscular layers of gastrointestinal smooth muscles and appear to contribute to the generation of pacemaker potentials in interstitial cells of Cajal from those tissues. However, the Ca^{2+} channel α subunit responsible for these currents has not been determined. We established that the α subunit of the α_{1H} Ca^{2+} channel is expressed in single myocytes and interstitial cells of Cajal using reverse transcription and polymerase chain reaction from whole tissue, laser capture microdissected tissue and single cells isolated from the mouse jejunum. Whole-cell voltage clamp recordings demonstrated that a nifedipine and Cd^{2+} resistant, mibefradil-sensitive current is present in myocytes dissociated from the jejunum. Electrical recordings from the circular muscle layer demonstrated that mibefradil reduced the frequency and initial rate of rise of the electrical slow wave. Gene targeted knockout of both alleles of the *cacna1h* gene, which encodes the α_{1H} Ca^{2+} channel subunit, resulted in embryonic lethality because of death of the homozygous knockouts prior to E13.5 days *in utero*. We conclude that a channel with the pharmacological and molecular characteristics of the α_{1H} Ca^{2+} channel subunit is expressed in interstitial cells of Cajal and myocytes from the mouse jejunum, and that ionic conductances through the α_{1H} Ca^{2+} channel contribute to the upstroke of the pacemaker potential. Furthermore, the survival of mice that do not express the α_{1H} Ca^{2+} channel protein is dependent on the genetic background and targeting approach used to generate the knockout mice.

Keywords: gastrointestinal motility • electrical slow wave • ion channels • transgenic animals

Introduction

T-type or low-voltage activated Ca^{2+} currents are detected in a variety of smooth muscle cells including gastrointestinal, vascular, myometrial and genito-urinary tract myocytes [1–4] where they are nearly always co-expressed with the L-type, high-voltage activated Ca^{2+} currents. Unlike L-type Ca^{2+} currents, the physiological roles of T-type Ca^{2+} currents are not clear although several studies have implicated these currents in regulation of rhythmic oscillations of membrane potential and control of myocyte proliferation during vascular development and remodelling [2].

The presence of low-voltage-activated, Ca^{2+} -permeable ionic conductances in cells from the external muscle layers of gastrointestinal smooth muscles has been reported in smooth muscle cells from the mouse colon [5], guinea pig taenia coli [6, 7], rat colon [3] and human colon [4] as well as interstitial cells of Cajal (ICC) from dog colon [8] and mouse colon and small intestine [9]. Many of these studies have identified the conductance as a T-type Ca^{2+} current [3, 4, 6, 7], and some of the other currents recorded in colonic myocytes have T-type properties [8, 9]. The physiological role of T-type Ca^{2+} currents in gastrointestinal myocytes has not been determined.

Data that do not support the presence of T-type Ca^{2+} channels in myocytes come from studies showing that inward Ca^{2+} permeable conductances recorded in myocytes from mouse colon are not as selective for Ca^{2+} as expected for T-type Ca^{2+} channels or are impermeable to Ba^{2+} . These data are consistent with the presence of an unclassified non-selective cation conductance in mouse colonic myocytes [5].

*Correspondence to: Simon J. GIBBONS,
Enteric Neuroscience Program, Mayo Clinic,
Guggenheim 838, 200 First Street SW,
Rochester MN 55905, USA.
Tel.: 507 284 4695
Fax: 507 284 0266
E-mail: gibbons.simon@mayo.edu

1 Together with enteric nerves and myocytes, interstitial cells of
2 Cajal (ICC) are required for normal gastrointestinal motility [10].
3 ICC generate the electrical slow wave; an oscillation in membrane
4 potential that is required for normal phasic contractions of gas-
5 trointestinal smooth muscles [11, 12] and a role for T-type Ca^{2+}
6 currents in the generation of slow waves has been proposed.
7 Normal slow wave activity results from Ca^{2+} influx through
8 plasma membrane ion channels, Ca^{2+} release from inositol 1,4,5-
9 trisphosphate sensitive Ca^{2+} stores, and re-polarization depen-
10 dent on a variety of ion channel types including non-selective cation
11 channels and/or Ca^{2+} activated Cl^- channels [13, 14]. The Ca^{2+}
12 influx that contributes to the upstroke of the electrical slow wave
13 is sensitive to block by agents that alter T-type Ca^{2+} channel
14 activity. Intracellular recordings from the external muscle layers of
15 mouse small intestine [15] indicate that a nifedipine-insensitive,
16 Ca^{2+} -permeable conductance is responsible for Ca^{2+} influx dur-
17 ing the electrical slow wave. In submucosal ICC from mouse
18 colon, Ni^{2+} (10–100 μM) and mibefradil (3 μM) application
19 resulted in a reduced rate of rise of the upstroke of the electrical
20 slow wave [16, 17]. Detailed analysis of the pacemaker potentials
21 and electrical slow waves recorded by impaling ICC and smooth
22 muscle cells in mouse small intestine showed that mibefradil
23 ($\geq 10 \mu\text{M}$) reduced the rate of rise of the upstroke depolarization
24 because of failure to entrain unitary potentials recorded from
25 ICC [18]. Experiments using imaging of intracellular Ca^{2+} transients
26 to follow pacemaker activity in myenteric ICC of human [19] and
27 mouse [20] small intestine, demonstrated that the upstroke phase
28 of the transient depends on activation of dihydropyridine-resistant
29 Ca^{2+} influx. In mouse ileum, this Ca^{2+} influx was blocked by low
30 concentrations of mibefradil (0.1 μM) and Ni^{2+} (100 μM) [20]
31 whereas in human small intestine [19], higher concentrations of
32 mibefradil (10–50 μM) were required to inhibit the Ca^{2+} influx.
33 These observations indicate that the conductance responsible for
34 the upstroke of the slow wave is probably a T-type Ca^{2+} current in
35 mouse but could be because of a different conductance in ICC of
36 the human small intestine [21].

37 The genes that encode three types of T-type Ca^{2+} channels
38 have been cloned from mouse and human tissue. These proteins,
39 $\text{Ca}_v3.1$, $\text{Ca}_v3.2$ and $\text{Ca}_v3.3$ (or α_{1G} , α_{1H} , and α_{1I} , respectively)
40 have the properties of T-type Ca^{2+} channels in heterologous
41 expression systems [22]. The messenger RNA (mRNA) for all
42 three T-type Ca^{2+} channels have been identified in mouse small
43 intestine by PCR but ICC of the deep muscular plexus (ICC-DMP)
44 do not express any T-type Ca^{2+} channel mRNA [23]. In mouse
45 colonic myocytes, α_{1G} complementary DNA (cDNA) could not be
46 amplified by reverse transcriptase polymerase chain reaction
47 (RT-PCR) [5].

48 For this study, we have further investigated whether T-type
49 Ca^{2+} currents play a role in the electrical properties of the mouse
50 jejunum based on the increased knowledge of the physiological
51 and pharmacological properties of the T-type Ca^{2+} current. We
52 have identified the T-type Ca^{2+} channel mRNA that is expressed in
53 myocytes and in ICC from the external muscle layers as α_{1H} and
54 we attempted to study the effect of knocking out expression of this
55 gene by gene-targeted mutagenesis.

Materials and methods

The Institutional Animal Care and Use Committee at Mayo Clinic, Rochester approved all animal handling procedures.

Harvest of tissue

Adult mice were killed by CO_2 inhalation followed by cervical dislocation. The small intestine was then rapidly removed and a 1–2 cm segment was rapidly frozen in liquid nitrogen to be cut into sections for laser capture microdissection. For RNA isolation, a longer 8–15 cm segment of jejunum was removed and placed in ice-cold, sterile Hanks balanced salt solution. The external muscle coat was rapidly peeled away from the mucosa and immediately placed in RNA later (Ambion Inc., Austin, TX, USA) for transfer to the molecular biology lab. For intracellular electrical recordings, a segment of small intestine wall, approximately 6 cm from the pylorus, was removed and placed in pre-oxygenated, normal Krebs solution at room temperature.

RNA isolation and reverse transcription and PCR amplification of cDNA

RNA was isolated from the external muscle coat of the adult mouse jejunum immediately after dissection as described previously for isolation of RNA from human jejunum smooth muscle [24].

Reverse-transcription PCR (RT-PCR)

PCR amplifications were performed using GeneAmp 2400 PCR Systems (PE Biosystems, Foster City, CA, USA) or iycler (Bio-Rad, Hercules, CA, USA) using standard procedures as previously published [24]. Reverse transcription (RT) was performed using a mixture of random hexamer and oligo dT primers following the instructions of the manufacturer (PE Biosystems). The product of the RT reaction was then amplified for T-type Ca^{2+} channel α subunits using gene specific primers that were specifically designed to flank regions containing introns in the genomic sequence (see Table 1 for details). All PCR products were purified and sent to the Mayo Molecular Core Facility for automated DNA sequencing.

Laser capture microdissection (LCM)

Sections of mouse jejunum, 6 μm thick, were mounted on glass slides and fixed in ice-cold acetone according to the protocol described previously [24]. A number of spots of tissue containing about 1500 smooth muscle cells from the circular muscle layer or the longitudinal muscle layer were collected using the PIX II Cell LCM system (Arcturus Engineering Inc., Santa Clara, CA, USA) with the 7.5- μm spot size. The caps with collected cells were then immediately placed into sterile 0.5 ml microcentrifuge tubes containing 300 μl RNA STAT-60 reagent (Tel-TEST Inc., Friendswood, TX, USA) for isolation of total RNA. After washing with 75% ethanol, the RNA pellet was resuspended in nuclease-free water (Ambion Inc.) and used for the RT-PCR.

Q3 Table 1

Target (Primer name)	Forward primer	Reverse primer	Expected size (bp)
PCR Primers			
Alpha 1H (YP1)	GCATGGCCTTCCTCACGTTGTT	GTGTAGTCTGGGATGCCGTCTT	697
(YP2)	TGCCGGTGGTGCCAAGATCCTA	GGCGCGTGTGTGAATAGTCTGC	628
Alpha 1G	CTACGGTCCCTTCGGCTACATT	TCCACTCGTATCTTCCCGTTTG	531
Alpha 1I	CTGTTTAGTCTGCGTGGGCTG	CTAACCAGACCCTCTCAGTC	608
Single cell PCR primers			
Alpha 1H (Outer)	CTTCTTGC GGCCATACTACC	CTGGTTTTCCCTCTGCTTTG	475
Alpha 1H (Inner)	TCACAATGGTGCCATCAACT	CTGGTTTTCCCTCTGCTTTG	232
Kit (Outer)	ATTATGAACGCCAGGAGACG	GAATCCCTCTGCCACACACT	497
Kit (Inner)	TACGAGGCCTACCCCAAACC	CTCTGCCACACACTGGAGCA	285
Genotyping primers			
Wild Type	AGGAGAGGCACTTACTGG	TAGGTATCAAGACTGTGAGG	487
Knockout	CGCAAGCCGGTGCCTGA	CCCTGTCTGAGTAGAACTG	520

Single cell PCR amplification from identified ICC

Single ICC from 3- to 5-day-old mice were obtained as previously described [25] from a dissociation of jejunal smooth muscle that had been immunolabelled with an antibody directly conjugated to the fluorophore Alexa 546 (Invitrogen). 3–5 labelled cells and 3–5 un-labelled, spindle-shaped cells were collected using a glass pipette and placed into an RNase free tube. A sample of bath solution was collected as a negative control against possible contamination. RNA was extracted then reverse transcribed using the ViLo Superscript III kit from Invitrogen. The cDNA was then probed for the presence of the α_{1H} Ca²⁺ channel transcript and c-Kit by two-step nested PCR using the primers shown in Table 1.

Generation of gene targeted knockout mice

Mice targeted for the knockout of the gene for the α_{1H} Ca²⁺ channel sub-unit by targeting the *Cacna1h* gene. The targeting vector was transfected into Lex-1 ES cells derived from 129SvEvBrd mice (Lexicon, The Woodlands, TX, USA) and the resulting clones were screened by PCR. Positively identified clones were injected into C57Bl/6 blastocysts and chimeric animals were bred to homozygosity.

Genotyping

Genotyping was done by Southern analysis using a probe (XP1) generated by PCR from genomic DNA. The genomic DNA was obtained from tails of the mice extracted using the Tissue Direct™ multiplex PCR system (GenScript, Piscataway, NJ, USA). EcoRI was used to digest 10 μ g of the genomic DNA for Southern blotting. The probe recognized a 11-kb fragment of wild-type DNA and a 9.5-kb fragment of DNA from the targeted allele.

PCR genotyping was also used to distinguish the wild-type and targeted alleles. The primers JLR5 and JLR6 were used to identify a 487 nucleotide band in the wild-type alleles and primers Puro3a and KO37 identified a 520 nucleotide band in the knockout allele (see Table 1 for primer sequences).

Intracellular electrical recordings

The segments of small intestine were opened along the anti-mesenteric border and transferred to a Petri dish filled with fresh oxygenated normal Krebs solution. The mucosa was removed under direct vision by using a binocular microscope and muscle strips (5 × 8 mm) were cut with the long axis parallel to the longitudinal muscle layer. Muscle strips were placed in a recording chamber and pinned with the serosal side down to a Sylgard-coated floor. The recording chamber had a volume of 1 ml and was perfused continuously with oxygenated normal Krebs solution at 37°C at a rate of 2 ml/min. The composition of the solution was (in mM) 137.4 Na⁺, 5.9 K⁺, 2.5 Ca²⁺, 1.2 Mg²⁺, 124 Cl⁻, 15.5 HCO₃⁻, 1.2 H₂PO₄⁻, and 11.5 glucose. It was continuously bubbled with 97% O₂, 3% CO₂, and maintained at pH 7.4.

Sharp glass microelectrodes filled with 3 M KCl (with input resistances ranging from 40 to 70 M Ω) were used to record intracellularly the membrane potential of smooth muscle cells. Approximately 30 min. before recording, 1 μ M nifedipine was added to reduce contractile activity of the muscle strip thereby facilitating long-term recordings from single cells. Recorded signals were amplified through an amplifier (Intra 767, WPI), digitized (Digidata 1322A, Axon Instruments), analyzed, and stored in a computer. When spontaneous electrical slow waves occurred, the membrane potential recorded between slow waves was considered the resting membrane potential (RMP). The time constant was measured as the time from the point at which the slow wave started to rise to the point the membrane potential reaches 63% of the maximum amplitude of the slow wave

1 cycle. Values are reported as mean \pm standard error (SEM). The Student's
2 t-test was used to compare mean slow wave frequency in control condi-
3 tions and during drug treatment. A P -value ≤ 0.05 was considered a sig-
4 nificant difference.

5 Whole-cell voltage clamp recordings

6
7
8
9 Currents were recorded from voltage clamped cells at 22°C using standard
10 whole-cell techniques [26, 27]. Microelectrodes were pulled from Kimble
11 KG-12 glass on a P-97 puller (Sutter Instruments, Novato, CA, USA).
12 Electrodes coated with R6101 (Dow Corning, Midland, MI, USA) were fire-
13 polished to a final resistance of 3–5 M Ω . Currents were amplified, digitized
14 and processed using an Axopatch 200B amplifier, Digidata 1322A, and
15 pCLAMP 9.2 software (Axon Instruments). Whole-cell records were sam-
16 pled at 10 kHz and filtered at 4 kHz with an 8-pole Bessel filter. During
17 analysis, the 0.1 ms (10 Hz) sampling interval of whole-cell records was
18 decimated 10-fold down to 1 ms (1 kHz). And 70–85% series resistance
19 compensation with a lag of 60 μ s was applied during each recording.
20 Freshly dissociated mouse intestinal smooth cells were held at a potential
21 of -100 mV and stepped from -80 to 35 mV in 5 mV intervals for 400 ms.
22 The start-to-start time was 516 ms.

23 Drug and solutions

24
25 The intracellular solution contained (in mM) 130 Cs⁺, 125 methanesul-
26 fonate, 20 Cl⁻, 5 Na⁺, 5 Mg²⁺, 5 HEPES, 2 EGTA, 2.5 ATP, and 0.1 GTP,
27 equilibrated to pH 7.0 (CsOH) with an osmolality 300 mmol/kg. Barium
28 currents were recorded in an extracellular solution containing (in mM) 80
29 Ba²⁺, 160 Cl⁻, and 5 HEPES, equilibrated to pH 7.35 (BaOH) and osmolal-
30 ity 297 mmol/kg (98.8 mM D-mannitol). To block L-type Ca²⁺ channels,
31 extracellular solutions were replaced with the same solution additionally
32 containing nifedipine (1 μ M, 1:10,000 ethanol:water) and/or CdCl₂
33 (30 μ M). Mibefradil (2.7 μ M) was used to block 50% of L-type Ca²⁺ and
34 90% of T-type Ca²⁺ channel current [28]. Chemicals and drugs were
35 purchased from Sigma-Aldrich Co. (St. Louis, MO, USA).

36 Data analysis

37
38 Patch clamp data were analyzed using Clampfit (MDS Inc., Union City, CA,
39 USA) and SigmaPlot (SPSS Inc., Chicago, IL, USA).

40 Results

41
42
43
44
45 The presence of mRNA for the T-type Ca channel α subunits, α_{1G} ,
46 α_{1H} and α_{1I} was investigated by reverse transcription and PCR of
47 total RNA derived from the external muscle layers of adult mouse
48 jejunum. Total RNA purified from mouse hippocampus was used
49 to provide a positive control for the effectiveness of the primers.
50 α_{1G} , and α_{1H} mRNA was amplified from the jejunum but although
51 α_{1I} transcripts were detected in the hippocampal samples, this
52 was not detected in samples from jejunum (Fig. 1A). The identity
53
54
55

of the products was confirmed by sequencing of the excised, puri-
fied products. We used the same primers to test whether any of
the transcripts were specifically expressed in cells from the circu-
lar smooth muscle layers of the gastric fundus and jejunum by
isolating cells using laser capture micro-dissection. α_{1H} mRNA
was amplified from all of the samples containing cells collected
from the jejunum but the primers for α_{1G} and α_{1I} did not amplify
products of the expected size in any of the jejunal LCM samples
(Fig. 1B). α_{1H} mRNA but not α_{1I} mRNA was also detected in cells
collected from the circular muscle layer of the gastric fundus. The
presence of α_{1G} mRNA in circular smooth muscle from the gastric
fundus was indicated by a faint band in one of the four gastric fun-
dus samples (Fig. 1B). PCR amplification from single cells was
used to further determine whether α_{1H} mRNA could be detected in
smooth muscle cells identified by their spindle shape and in ICC
identified by Kit immunoreactivity. A product that was confirmed
by sequencing to be amplified from α_{1H} mRNA was detected in all
of the tubes ($n = 5$ tubes) that contained either smooth muscle
cells or Kit-positive ICC (examples shown in Fig. 1C). c-Kit mRNA
was amplified from tubes containing Kit immunoreactive cells but
was not amplified from tubes containing Kit-negative, spindle
shaped cells (Fig. 1C) confirming the identity of the collected cells.
Representative PCR results are shown for a sample containing Kit-
positive cells (S1) and Kit-negative cells (S2) as well as results
from a separate RT-PCR reaction using Kit-positive cells (S3) and
bath solution. A product was not amplified from a tube containing
the bath water.

The presence of α_{1H} transcripts in cells from mouse jejunum
smooth muscle suggested that cells from this region may express
mibefradil-sensitive, nifedipine and Cd²⁺-resistant T-type Ca²⁺
channels. To verify this, we did whole-cell voltage clamp record-
ings on freshly dissociated myocytes from the mouse jejunum
(Fig. 2). In the presence of 1 μ M nifedipine and 80 mM Ba²⁺, an
inward current was recorded that was inhibited by more than 90%
with 2.7 μ M mibefradil (Fig. 2A). This rapidly inactivating current
activated at -50 mV with a peak inward current at -5 mV
(Fig. 2A(ii)). Cadmium (30 μ M), expected to block L-type but not
T-type Ca²⁺ channels, did not block the current and this Cd²⁺-
resistant current was also inhibited by more than 90% with
2.7 μ M mibefradil (Fig. 2B).

The molecular and functional evidence for T-type Ca²⁺ chan-
nels in the mouse jejunum prompted us to investigate whether
inhibitors of T-type Ca²⁺ channels would affect the electrical slow
wave in mouse jejunum. When studying balb/c wild-type mice,
mibefradil, at a concentration that will predominantly block T-type
Ca²⁺ channels (2 μ M, [28]), did not completely block the slow
wave. However, the time constant for the rising phase of the elec-
trical slow wave was increased from 0.093 ± 0.005 sec. ($n = 9$
cells from five mice) to 0.171 ± 0.015 sec. ($n = 10$ cells from
three mice, $P < 0.01$) and the frequency of electrical slow waves
was reduced from 0.67 ± 0.02 Hz to 0.59 ± 0.02 ($P < 0.05$).
Mibefradil had no significant effect on the resting membrane
potential of the impaled smooth muscle cells (-64.7 ± 2.9 mV in
control, -69.2 ± 2.6 mV in mibefradil, $P = 0.26$) (Fig. 3).

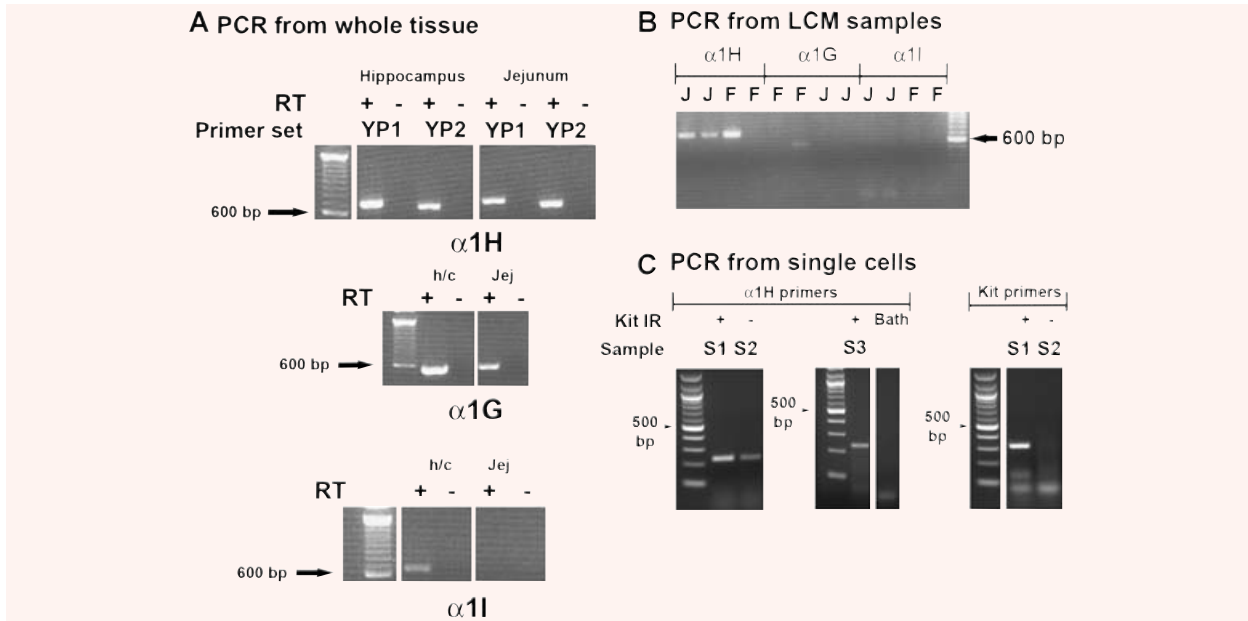


Fig. 1 (A) PCR amplification of T-type Ca^{2+} channel α subunit mRNA from the external muscle layers of adult mouse jejunum. Amplification from hippocampal mRNA is shown as a positive control. YP1 and YP2 represent two different primer sets (see Table 1 for details). (B) PCR amplification of T-type Ca^{2+} channel α subunit mRNA from smooth muscle cells from wild-type (WT) mouse jejunum and fundus that were collected by laser capture micro-dissection (LCM). (C) Representative PCR amplifications of T-type Ca^{2+} channel α subunit mRNA from single tubes of Kit immunoreactive (Kit-IR, S1 and S3) and Kit-negative spindle-shaped cells (S2). A sample of the bath solution (BATH) was also collected and subjected to RT-PCR as a negative control. Primers were designed against the T-type Ca^{2+} channel subunit covering at least one intron to avoid genomic contamination. The specific products for α_{1H} were amplified by reverse transcription PCR (RT-PCR). J = jejunum; F = fundus, RT = control for genomic contamination, *i.e.* under-vent RT-PCR in the absence of reverse transcriptase. A 100 bp DNA ladder was loaded and is shown to indicate product size.

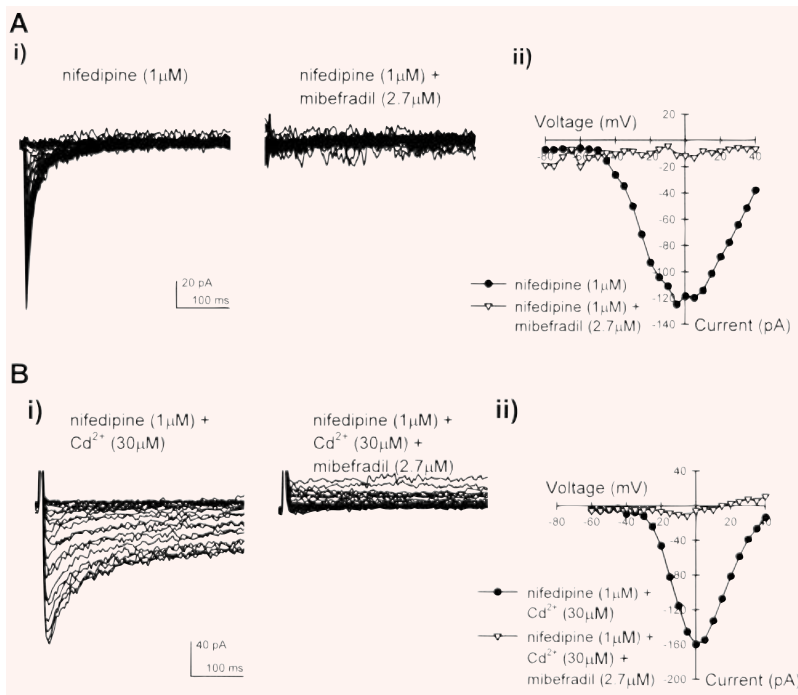


Fig. 2 Representative T-type whole-cell currents recorded in myocytes from the outer muscle layers of the mouse jejunum. (A) (i) Nifedipine-resistant, mibefradil-sensitive Ba^{2+} currents, (ii) Current-voltage relationship for the peak inward currents shown in (A) (i). (B) (i) Mibefradil-sensitive Ba^{2+} currents obtained in the presence of nifedipine and Cd^{2+} , (ii) Current-voltage relationship for the peak inward currents shown in (B) (i). Currents were recorded by stepping the command voltage from -100 mV to between -80 and $+35$ mV in 5 mV steps.

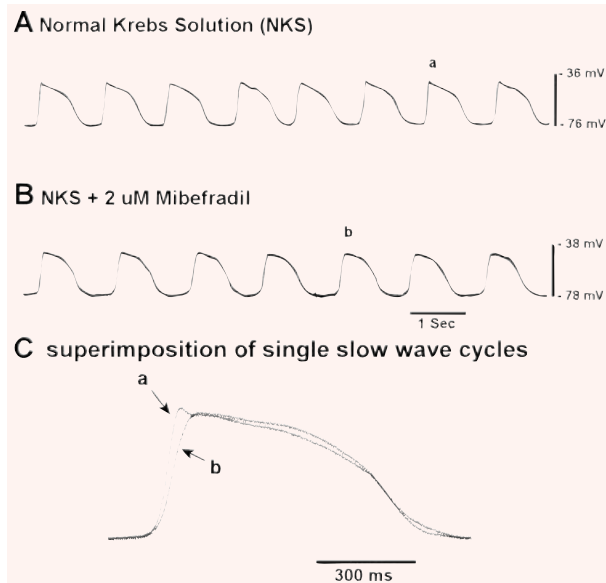


Fig. 3 Mibefradil reduces the initial rate of rise and frequency of the electrical slow wave in the circular smooth muscle layer of the mouse jejunum. **(A)** Control recording, **(B)** recording in the presence of 2 μ M mibefradil **(C)** superimposition of single slow wave cycles to show the effect of mibefradil.

To further examine the contribution of α_{1H} T-type Ca^{2+} channel subunits on gastrointestinal smooth muscle function, we attempted to knock out expression of the functional protein by targeting the gene for α_{1H} , *cacna1h*. The targeting vector was designed to disrupt exons 3 to 6 of the genomic sequence as shown in Fig. 4A. This region corresponds to amino acid residues 138 to 373 in the expressed protein. Southern analysis of genomic DNA obtained from tails of heterozygous animals and digested using EcoRI detected an 11 kb wild-type band and a 9.5-kb targeted band when using the external probe XP1, as shown in Fig. 4B. Examples of Southern blots from wild-type and heterozygous mice are shown in Fig. 4B. Genotyping was also done by PCR using the primers JLR5 and JLR6 to identify the wild-type allele and Puro3a and KO37 to identify the knockout allele. Mice heterozygous for the knockout allele survived, had no obvious phenotype and had no problems with breeding. However, only one mouse homozygous for the knockout allele was identified by either PCR or Southern blot as shown in Table 1 (see also Fig. 4B for examples).

In total, more than 200 adult mice were tested for genotype without identifying a homozygous knockout animal, so we examined the proportions of the alleles in mice generated from 10 separate pairs of heterozygous animals. The proportions of the genotypes of the mice obtained from breeding heterozygotes (Table 2), significantly deviated from the proportions predicted by Hardy Weinberg principles ($P < 0.0001$, χ^2 test) indicating that the homozygous knockout animals were dying prior to genotyping. We saw no evidence of pups dying shortly after birth. Therefore,

we reasoned that the homozygous mutant animals were dying *in utero*. We tested whether the homozygous knockouts were dying before birth by mating four heterozygous pairs of mice. The females were killed at fixed times from the detection of vaginal plugs and the foetuses removed under sterile conditions. The foetuses were photographed and then tissue from the head was removed for DNA extraction and genotyping. The proportions of the genotypes deviated significantly from Hardy Weinberg proportions ($P = 0.0015$, χ^2 test) and no foetuses homozygous for the mutated allele were detected in female mice more than 10.5 days after the plug was detected (Table 1). However, foetuses homozygous for the knockout allele were detected before embryonic day 10.5 in numbers that did not deviate significantly from Hardy Weinberg proportions ($P > 0.05$, χ^2 test, Table 1). The foetuses did not have anatomical abnormalities that allowed us to distinguish between knockout and heterozygous or wild-type animals at embryonic age 9.5 to 10.5 (Fig. 5). The hearts were beating when the foetuses were removed and there were no clear neural tube defects. However, later during gestation (E17.5 to E19.5) reabsorbed foetuses were observed in the uteruses removed for genotyping of the foetuses.

We were unable to obtain more than one mouse that was homozygous for the knockout allele so we compared the properties of the electrical slow wave in the circular smooth muscle layer from the jejunum of four mice heterozygous for the knockout with the properties in four wild-type siblings. Forty-one cells from heterozygous mutant mice and 39 cells from wild-type mice were studied and no differences were detected in the rate of rise of the electrical slow wave as (Time constant in heterozygous animals = 0.143 ± 0.007 sec, homozygous wild type = 0.139 ± 0.006 sec., $P > 0.05$). The electrical slow wave recorded from smooth muscle cells in the jejunum in the one mouse homozygous for knockout of the α_{1H} gene appeared abnormal. The slope of the initial rising phase of the slow wave was lower than usual and the frequency of the slow waves was less than half the normal value (0.296 ± 0.009 Hz, $n = 7$ cells, Fig. 6 versus 0.67 ± 0.02 Hz in 9 cells from 5 balb/c wild-type mice, see above) with no clear difference in the resting membrane potential of the cells (-56.1 ± 2.3 mV, $n = 7$ cells versus -64.7 ± 2.9 mV in 9 cells from 5 balb/c wild-type mice, see above).

Discussion

Inward cationic conductances that are activated at comparatively negative membrane potentials (< -30 mV) and that are not selectively permeable, or are permeable to Ca^{2+} or Na^+ , have been demonstrated in gastrointestinal smooth muscle cells and interstitial cells of Cajal from many species [3–9, 24, 29]. As a result of recent pharmacological and technical advances, the biophysical and molecular identification of these conductances should be possible but so far few have been definitively identified [24]. In this study, we have demonstrated the expression of the α_{1H} Ca^{2+}

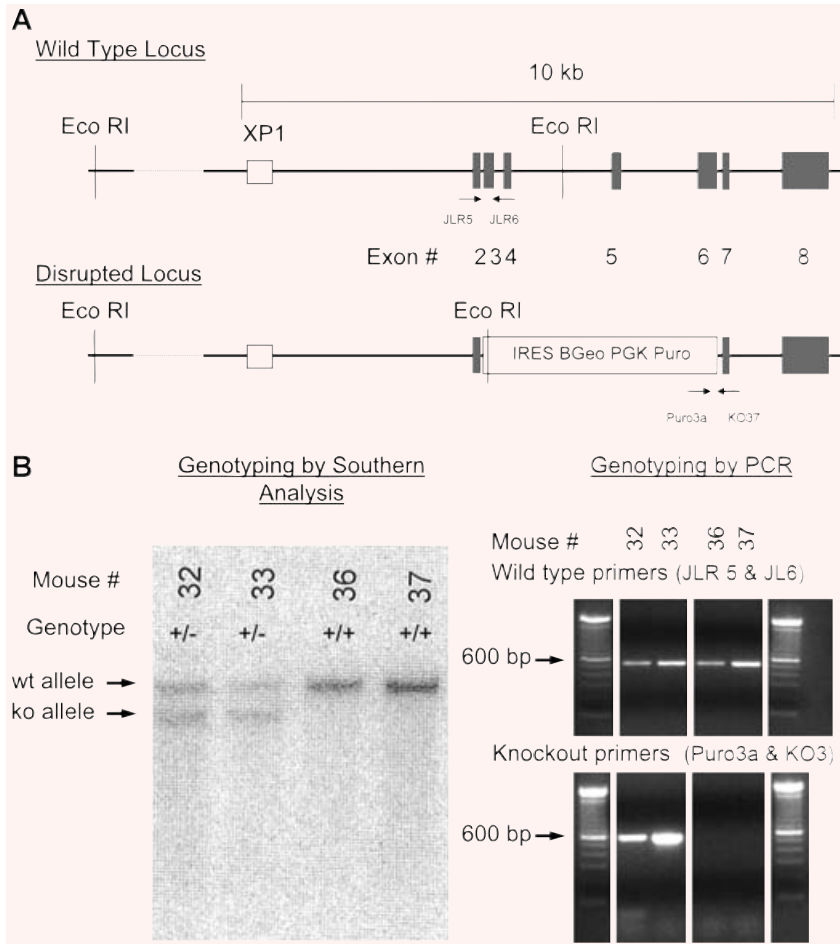


Fig. 4 Gene targeted knockout of the α_{1H} Ca^{2+} channel subunit in mice. **(A)** Schematic of the wild-type and disrupted alleles showing the distribution of exons 2 to 8, the location of the key EcoR1 restriction sites for Southern blot analysis. The location of the binding sites for the Southern blot probe (XP1) and the oligonucleotide PCR primers for identifying the wild-type (JLR5 and JLR6) and disrupted (Puro3a and KO37) alleles are also shown. A 100 bp DNA ladder was loaded and is shown to indicate product size. **(B)** An example of Southern blot analysis of the alleles present in the genomes of four mice is shown together with PCR confirmation of the genotype using DNA samples from the same mice.

Table 2 Genotypes of mice resulting from mating of pairs of heterozygous animals

	Post-natal	Embryonic age	Embryonic age
		E17.5 to E19.5	E9.5 to E10.5
Wild type	26 (33%)	3 (16%)	2 (10%)
Heterozygous	54 (66%)	16 (84%)	10 (47%)
Homozygous	1	0	9
Knockout	(1%)	(0%)	(43%)
Number of litters	10	2	2

channel subunit in the circular smooth muscle layer of the mouse jejunum and fundus, specifically in myocytes and ICC from the jejunum. We have also determined that inhibition of T-type Ca^{2+} currents affects the electrical slow wave in this tissue. We did not

directly record from identified ICC in this article and attempts to directly determine the contribution of the α_{1H} subunit to gastrointestinal function were not successful because of the lethal effects of knocking out the *cacna1h* gene, which encodes this protein.

The problems with dissecting out Ca^{2+} currents in myocytes and ICC are that some of the T-type Ca^{2+} channels are quite resistant to the effect of Ni^{2+} ($> 200 \mu M$ for α_{1I} and α_{1G} , [30]) and Ni^{2+} has effects on other Ca^{2+} permeable channels or transporters in the plasma membrane [31–34]. When used at the correct concentration, mibefradil is a fairly selective inhibitor of T-type Ca^{2+} channels [35] with a 4- to 10-fold higher potency as an inhibitor of T-type Ca^{2+} channels when compared to its effects on L-type Ca^{2+} channels and the sodium channel, $Na_v1.5$ [28] but it is often tested at concentrations that are not selective and its effects are diminished at positive membrane voltages [36]. Similarly, excluding the other Ca^{2+} permeable conductances in the cells can be difficult because of the lack of selective inhibitors of non-selective cation conductances. When L-type Ca^{2+} currents are present in the cells, these currents can be inhibited by dihydropyridine calcium channel blockers but the effectiveness of dihydropyridines is reduced at the more negative membrane

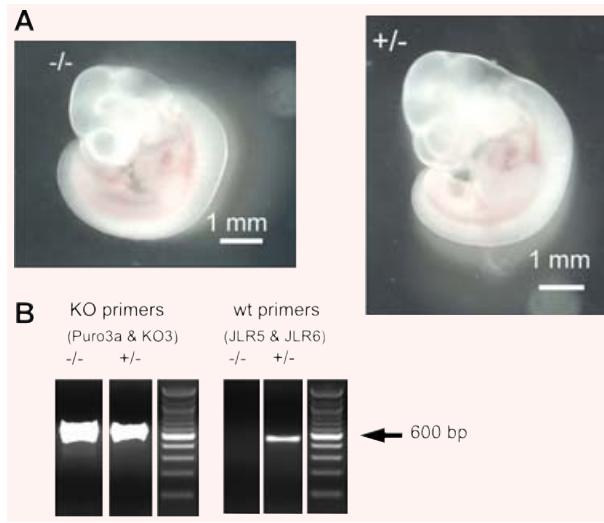


Fig. 5 Foetuses homozygous or heterozygous for the knockout of the *cacna1h* gene exhibit no gross abnormalities. (A) Images of foetuses obtained 9 days after detection of a vaginal plug (E9.5). (B) Results of PCR genotyping of the foetuses shown. (KO = knockout, wt = wild type). A 100 bp DNA ladder was loaded and is shown to indicate product size.

voltages [37] where the low-voltage activated current is observed, possibly leading to the erroneous identification of residual L-type current as a low-voltage activated Ca^{2+} current. In addition dihydropyridines inhibit some T-type Ca^{2+} channels at concentrations greater than $5 \mu\text{M}$ [38].

The molecular identification of the α_{1H} subunit in mouse jejunal smooth muscle is consistent with the biophysical and pharmacological properties of the low-voltage activated Ca^{2+} selective conductance reported herein in mouse jejunal myocytes and recorded by several groups in smooth muscle cells from rat small intestine [3] as well as myocytes from other gastrointestinal tissue [3, 6–9]. Specifically, the α_{1H} Ca^{2+} channel subunit is resistant to inhibition by nifedipine and Cd^{2+} and is blocked by mibefradil at $2.7 \mu\text{M}$ [35]. Other distinguishing properties of the α_{1H} Ca^{2+} channel subunit are activation starting at -60 mV and similar relative selectivity and permeability to Ca^{2+} and Ba^{2+} ions.

None of the previously published studies on the expression of T-type Ca^{2+} channel α subunits have tested for the presence of the α_{1H} subunit and none have identified a candidate for the low-voltage activated cation conductance in myocytes from rodent circular smooth muscle [5, 23]. In one study, mRNA for the α_{1G} subunit was not detected in myocytes from mouse colonic circular muscle [5]. In the other study, the presence was demonstrated of all three T-type Ca^{2+} channel α subunits in the external muscle layers of mouse small intestine but this study did not determine if myocytes expressed the mRNA for any of the subunits. We could not detect the α_{1I} subunit mRNA in our samples even though the primers worked in our positive control experiment. Three different primer sets were tested for the α_{1I} subunit

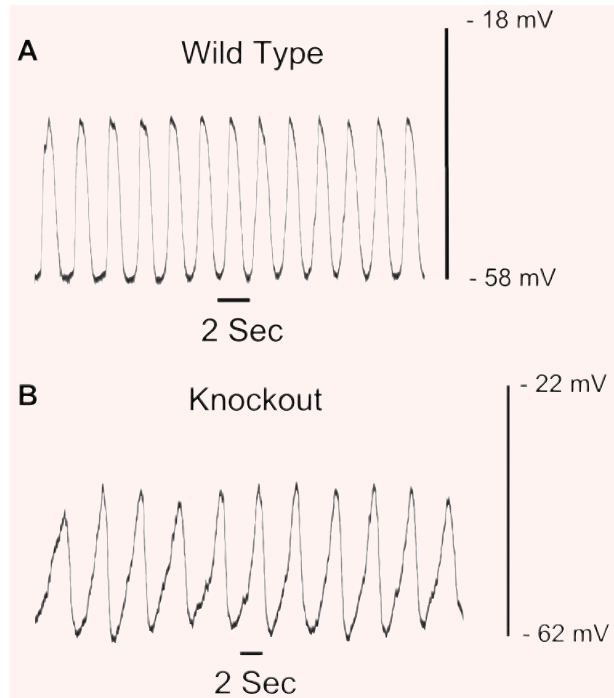


Fig. 6 The initial rate of rise and frequency of the electrical slow wave recorded in the circular smooth muscle layer of the mouse jejunum are lower in a mouse homozygous for the α_{1H} knockout. (A) Control recording from a wild-type balb/c mouse, (B) Recording from a homozygous knockout mouse.

and none amplified a product of the expected size (data not shown). One possible explanation for the amplification of α_{1H} Ca^{2+} channel mRNA from the circular smooth muscle layer of the mouse jejunum is that the mRNA came from a cell type other than the myocytes or ICC. In human myometrium, α_{1H} Ca^{2+} channel immunoreactivity was detected in lymphocytes but not smooth muscle cells [1]. This is consistent with a role for T-type Ca^{2+} channels in the migration of leucocytes [39]. However, the samples that we collected by laser capture microdissection were from histochemically stained sections and were taken from the circular smooth muscle layer in regions that did not show evidence of lymphocytic contamination. In addition, the single cells that we collected were either Kit-immunoreactive or had myocyte morphology, so we consider it unlikely that this could account for the results.

The reduction in the rate of rise of the electrical slow wave recorded in myocytes of mouse jejunum in response to mibefradil treatment is consistent with an effect of mibefradil on ICC as previously published in other tissues. The upstroke of electrical slow waves recorded in mouse small intestine involves Ca^{2+} influx through a non-L type Ca^{2+} channel [15], Ni^{2+} ($1\text{--}100 \mu\text{M}$) reduces the rate of rise of slow waves in guinea pig gastric antrum [40] and the upstroke of pacemaker potentials in mouse ICC recorded by Ca^{2+} imaging was inhibited by mibefradil ($0.1 \mu\text{M}$)

and Ni^{2+} (100 μM) [20]. These experimental results are further supported by mathematical models of pacemaker potentials in ICC that show the necessity for a voltage activated Ca^{2+} current in order to accurately model the pacemaker potentials. [41]. Interestingly, slowing of the rise time for the electrical slow wave in mice in mibefradil and Ni^{2+} is similar to the effects of inhibiting the tetrodotoxin (TTX)-resistant Na^+ channel, $\text{Na}_v1.5$ on the electrical slow wave recorded in circular muscle of human jejunum [29]. Also, mibefradil and Ni^{2+} do not completely block the upstroke at concentrations where near complete inhibition of a T-type channel is expected [18] suggesting the possibility that more than one channel type may contribute to the upstroke. These pharmacological properties also raise the possibility that the observed current carried by non-L-type Ca^{2+} channels is carried by T-type-like channels and the possibility that the current is carried by a combination of alpha subunits or a novel T-type alpha subunit cannot be excluded.

The target for mibefradil is likely the α_{1H} channel subunit identified in ICC by single cell PCR rather than in smooth muscle because the electrical slow wave is generated by ICC in the myenteric plexus region of the mouse jejunum, where the pacemaker potential is initiated. As the slow wave is generated by ICC, there should not be a need for a T-type Ca^{2+} channel to participate in the generation of the upstroke in smooth muscle cells. It may be that Ca^{2+} influx through T-type Ca^{2+} channels in myocytes is more important for functions of Ca^{2+} unrelated to contractility such as cellular proliferation or migration. In this respect, myocytes from mouse jejunum are similar to other smooth muscles [2, 42] although there does appear to be role for α_{1H} Ca^{2+} channel subunits in controlling relaxation of coronary smooth muscle [43].

Studies in the mice heterozygous for the knockout of the α_{1H} Ca^{2+} channel subunit did not provide any further information because when compared with wild-type litter-mates, there were no differences in the properties of the electrical slow wave. This indicates that the partial knockout did not have a gene dosing effect.

The lethal effects of knocking out expression of the α_{1H} Ca^{2+} channel subunit in all but one of the many hundreds of mice studied were surprising given that another group has successfully generated a strain of mice by deletion of exon 6 in the *cacna1h*

gene [43]. The reported effects of this knockout were cardiac injury because of coronary artery constriction and reduced body mass compared to wild-type litter mates. These are both phenotypes consistent with reduced survival but were clearly not sufficient to prevent survival to maturity of the knockout mice [43]. We were only able to obtain one adult mouse homozygous for the knockout allele over a period of 4 years studying these animals and we conclude that this very low survival rate reflects the genetic backgrounds of the strain of either embryonic stem cells or recipient blastocysts [44]. We could not identify the actual cause of death of the homozygous knockout fetuses but death of fetuses at ages around E10.5 is associated with cardiovascular abnormalities (*e.g.* [45], and this is consistent with both the phenotype of the published α_{1H} knockout [43] and the known role of T-type Ca^{2+} channels in smooth muscle cell growth and proliferation [2]. Neural tube abnormalities, which also can cause embryonic lethality at around E10.5 [46], were not observed. Interestingly, the rate of rise and frequency of the electrical slow wave were lower than normal values in recordings from the jejunum of the one mouse that did survive.

In conclusion, the α_{1H} Ca^{2+} channel subunit is expressed in myocytes and ICC from the circular muscle layer of mouse jejunum. A T-type Ca^{2+} current also appears to play a role in the generation of the upstroke of the electrical slow wave in mouse tissue and the pharmacological properties of this current are consistent with expression of the α_{1H} Ca^{2+} channel subunit in ICC contributing to this current. The phenotypic effect of knocking out the gene for the α_{1H} Ca^{2+} channel subunit is dependent on the genetic background of the mouse strain used for the construct and can be embryonic lethal in some mouse strains.

Acknowledgements

We thank Dr. Stephen Thibodeau (and his lab) for their assistance with the Southern blots and Dr. Jan Van Deursen (and his lab, especially Darren Baker) for their assistance with dissecting out the mouse embryos. This work was supported by the following grants from the NIH, DK 52766, DK 57061 and DK 68055.

References

- Blanks AM, Zhao ZH, Shmygol A, Bru-Mercier G, Astle S, Thornton S. Characterization of the molecular and electrophysiological properties of the T-type calcium channel in human myometrium. *J Physiol.* 2007; 581: 915–26.
- Cribbs LL. T-type Ca^{2+} channels in vascular smooth muscle: multiple functions. *Cell Calcium.* 2006; 40: 221–30.
- Xiong Z, Sperelakis N, Noffsinger A, Fenoglio-Preiser C. Changes in calcium channel current densities in rat colonic smooth muscle cells during development and aging. *Am J Physiol.* 1993; 265: C617–25.
- Xiong Z, Sperelakis N, Noffsinger A, Fenoglio-Preiser C. Ca^{2+} currents in human colonic smooth muscle cells. *Am J Physiol.* 1995; 269: G378–85.
- Koh SD, Monaghan K, Ro S, Mason HS, Kenyon JL, Sanders KM. Novel voltage-dependent non-selective cation conductance in murine colonic myocytes. *J Physiol.* 2001; 533: 341–55.
- Yamamoto Y, Hu SL, Kao CY. Inward current in single smooth muscle cells of the guinea pig taenia coli. *J Gen Physiol.* 1989; 93: 521–50.
- Yoshino M, Someya T, Nishio A, Yazawa K, Usuki T, Yabu H. Multiple types of voltage-dependent Ca channels in mammalian intestinal smooth muscle cells. *Pflugers Arch.* 1989; 414: 401–9.

- 1 8. **Lee HK, Sanders KM.** Comparison of ionic
2 currents from interstitial cells and smooth
3 muscle cells of canine colon. *J Physiol.*
4 1993; 460: 135–52.
- 5 9. **Kim YC, Koh SD, Sanders KM.** Voltage-
6 dependent inward currents of interstitial
7 cells of Cajal from murine colon and
8 small intestine. *J Physiol.* 2002; 541:
9 797–810.
- 10 10. **Farrugia G.** Interstitial cells of Cajal in
11 health and disease. *Neurogastroenterol*
12 *Motil.* 2008; 20: 54–63.
- 13 11. **Huizinga JD, Thuneberg L, Kluppel M,**
14 **Malysz J, Mikkelsen HB, Bernstein A.**
15 **W/kit gene required for interstitial cells of**
16 **Cajal and for intestinal pacemaker activity.**
17 *Nature.* 1995; 373: 347–9.
- 18 12. **Ward SM, Burns AJ, Torihashi S, Sanders**
19 **KM.** Mutation of the proto-oncogene c-kit
20 blocks development of interstitial cells and
21 electrical rhythmicity in murine intestine. *J*
22 *Physiol.* 1994; 480: 91–7.
- 23 13. **Huizinga JD, Zhu Y, Ye J, Molleman A.**
24 **High-conductance chloride channels gener-**
25 **ate pacemaker currents in interstitial**
26 **cells of Cajal.** *Gastroenterology.* 2002; 123:
27 1627–36.
- 28 14. **Sanders KM, Koh SD, Ward SM.**
29 **Interstitial cells of Cajal as pacemakers in**
30 **the gastrointestinal tract.** *Annu Rev*
31 *Physiol.* 2006; 68: 307–43.
- 32 15. **Malysz J, Richardson D, Farraway L,**
33 **Christen MO, Huizinga JD.** Generation of
34 slow wave type action potentials in the
35 mouse small intestine involves a non-L-
36 type calcium channel. *Can J Physiol*
37 *Pharmacol.* 1995; 73: 1502–11.
- 38 16. **Hotta A, Okada N, Suzuki H.** Mibefradil-
39 sensitive component involved in the
40 plateau potential in submucosal interstitial
41 cells of the murine proximal colon. *Biochem*
42 *Biophys Res Commun.* 2007; 353:
43 170–6.
- 44 17. **Yoneda S, Takano H, Takaki M, Suzuki H.**
45 **Effects of nifedipine and nickel on plateau**
46 **potentials generated in submucosal inter-**
47 **stitial cells distributed in the mouse prox-**
48 **imal colon.** *J Smooth Muscle Res.* 2003;
49 39: 55–65.
- 50 18. **Kito Y, Ward SM, Sanders KM.** Pacemaker
51 potentials generated by interstitial cells of
52 Cajal in the murine intestine. *Am J Physiol*
53 *Cell Physiol.* 2005; 288: C710–20.
- 54 19. **Lee HT, Hennig GW, Fleming NW, Keef**
55 **KD, Spencer NJ, Ward SM, Sanders KM,**
Smith TK. The mechanism and spread of
pacemaker activity through myenteric
interstitial cells of Cajal in human small
intestine. *Gastroenterology.* 2007; 132:
1852–65.
20. **Park KJ, Hennig GW, Lee HT, Spencer**
NJ, Ward SM, Smith TK, Sanders KM.
Spatial and temporal mapping of pace-
maker activity in interstitial cells of Cajal in
mouse ileum *in situ.* *Am J Physiol Cell*
Physiol. 2006; 290: C1411–27.
21. **Farrugia G.** Ca²⁺ handling in human inter-
stitial cells of Cajal. *Gastroenterology.*
2007; 132: 2057–9.
22. **Perez-Reyes E.** Molecular characterization
of T-type calcium channels. *Cell Calcium.*
2006; 40: 89–96.
23. **Chen H, Redelman D, Ro S, Ward SM,**
Ordog T, Sanders KM. Selective labeling
and isolation of functional classes of inter-
stitial cells of Cajal of human and murine
small intestine. *Am J Physiol Cell Physiol.*
2007; 292: C497–507.
24. **Ou Y, Gibbons SJ, Miller SM, Strege PR,**
Rich A, Distad MA, Ackerman MJ, Rae
JL, Szurszewski JH, Farrugia G. SCN5A is
expressed in human jejunal circular
smooth muscle cells. *Neurogastroenterol*
Motil. 2002; 14: 477–86.
25. **Wouters MM, Gibbons SJ, Roeder JL,**
Distad M, Ou Y, Strege PR, Szurszewski
JH, Farrugia G. Exogenous serotonin reg-
ulates proliferation of interstitial cells of
Cajal in mouse jejunum through 5-HT_{2B}
receptors. *Gastroenterology.* 2007; 133:
897–906.
26. **Farrugia G, Irons WA, Rae JL, Sarr MG,**
Szurszewski JH. Activation of whole cell
currents in isolated human jejunal circular
smooth muscle cells by carbon monoxide.
Am J Physiol. 1993; 264: G1184–9.
27. **Farrugia G, Rae JL, Szurszewski JH.**
Characterization of an outward potassium
current in canine jejunal circular smooth
muscle and its activation by fenamates. *J*
Physiol. 1993; 468: 297–310.
28. **Strege PR, Bernard CE, Ou Y, Gibbons**
SJ, Farrugia G. Effect of mibefradil on
sodium and calcium currents. *Am J*
Physiol Gastrointest Liver Physiol. 2005;
289: G249–53.
29. **Strege PR, Ou Y, Sha L, Rich A, Gibbons**
SJ, Szurszewski JH, Sarr MG, Farrugia G.
Sodium current in human intestinal inter-
stitial cells of Cajal. *Am J Physiol*
Gastrointest Liver Physiol. 2003; 285:
G1111–21.
30. **Lee JH, Gomora JC, Cribbs LL, Perez-**
Reyes E. Nickel block of three cloned T-
type calcium channels: low concentrations
selectively block alpha1H. *Biophys J.*
1999; 77: 3034–42.
31. **Chaib N, Kabre E, Metioui M, Alzola E,**
Dantinne C, Marino A, Dehaye JP.
Differential sensitivity to nickel and
SK&F96365 of second messenger-oper-
ated and receptor-operated calcium chan-
nels in rat submandibular ductal cells. *Cell*
Calcium. 1998; 23: 395–404.
32. **Hinde AK, Perchenet L, Hobai IA, Levi**
AJ, Hancox JC. Inhibition of Na/Ca
exchange by external Ni in guinea-pig ven-
tricular myocytes at 37 degrees C, dialysed
internally with cAMP-free and cAMP-con-
taining solutions. *Cell Calcium.* 1999; 25:
321–31.
33. **Kimura J, Miyamae S, Noma A.**
Identification of sodium-calcium exchange
current in single ventricular cells of
guinea-pig. *J Physiol.* 1987; 384: 199–
222.
34. **Ng LC, Gurney AM.** Store-operated chan-
nels mediate Ca(2⁺) influx and contraction
in rat pulmonary artery. *Circ Res.* 2001;
89: 923–9.
35. **Martin RL, Lee JH, Cribbs LL, Perez-**
Reyes E, Hanck DA. Mibefradil block of
cloned T-type calcium channels. *J*
Pharmacol Exp Ther. 2000; 295: 302–8.
36. **Bezprozvanny I, Tsien RW.** Voltage-
dependent blockade of diverse types of
voltage-gated Ca²⁺ channels expressed in
Xenopus oocytes by the Ca²⁺ channel
antagonist mibefradil (Ro 40–5967). *Mol*
Pharmacol. 1995; 48: 540–9.
37. **Bean BP.** Nitrendipine block of cardiac cal-
cium channels: high-affinity binding to the
inactivated state. *Proc Natl Acad Sci USA.*
1984; 81: 6388–92.
38. **Shcheglovitov A, Zhelay T, Vitko Y,**
Osipenko V, Perez-Reyes E, Kostyuk
P, Shuba Y. Contrasting the effects of
nifedipine on subtypes of endogenous
and recombinant T-type Ca²⁺ chan-
nels. *Biochem Pharmacol.* 2005; 69:
841–54.
39. **Nebe B, Holzhausen C, Rychly J,**
Urbaszek W. Impaired mechanisms of
leukocyte adhesion *in vitro* by the calcium
channel antagonist mibefradil. *Cardiovasc*
Drugs Ther. 2002; 16: 183–93.
40. **Tomita T, Pang YW, Ogino K.** The effects
of nickel and cobalt ions on the sponta-
neous electrical activity, slow wave, in the
circular muscle of the guinea-pig gastric
antrum. *J Smooth Muscle Res.* 1998; 34:
89–100.
41. **Faville RA, Pullan AJ, Sanders KM,**
Smith NP. A biophysically based mathe-
matical model of unitary potential activity
in interstitial cells of Cajal. *Biophys J.*
2008; 95: 88–104.
42. **Fry CH, Sui G, Wu C.** T-type Ca²⁺ chan-
nels in non-vascular smooth muscles. *Cell*
Calcium. 2006; 40: 231–9.

- 1
2
3
4
5
6
7
8
9
10
11
12
13
14
15
16
17
18
19
20
21
22
23
24
25
26
27
28
29
30
31
32
33
34
35
36
37
38
39
40
41
42
43
44
45
46
47
48
49
50
51
52
53
54
55
43. **Chen CC, Lamping KG, Nuno DW, Barresi R, Prouty SJ, Lavoie JL, Cribbs LL, England SK, Sigmund CD, Weiss RM, Williamson RA, Hill JA, Campbell KP.** Abnormal coronary function in mice deficient in alpha1H T-type Ca²⁺ channels. *Science*. 2003; 302: 1416–8.
44. **Gerlai R.** Gene-targeting studies of mammalian behavior: is it the mutation or the background genotype? *Trends Neurosci*. 1996; 19: 177–81.
45. **Takehima H, Komazaki S, Hirose K, Nishi M, Noda T, Iino M.** Embryonic lethality and abnormal cardiac myocytes in mice lacking ryanodine receptor type 2. *EMBO J*. 1998; 17: 3309–16.
46. **Harris MJ, Juriloff DM.** Mini-review: toward understanding mechanisms of genetic neural tube defects in mice. *Teratology*. 1999; 60: 292–305.